

# Validity of Retinal Oxygen Saturation Analysis: Hyperspectral Imaging in Visible Wavelength with Fundus Camera and Liquid Crystal Wavelength Tunable Filter

Yoko HIROHARA<sup>1,2</sup>, Yoshitaka OKAWA<sup>1</sup>, Toshifumi MIHASHI<sup>1,2</sup>, Tatsuo YAMAGUCHI<sup>2</sup>, Naoki NAKAZAWA<sup>2</sup>, Yasuko TSURUGA<sup>2</sup>, Hiroyuki AOKI<sup>2</sup>, Naoyuki MAEDA<sup>3</sup>, Ichiro UCHIDA<sup>4</sup>, and Takashi FUJIKADO<sup>1\*</sup>

<sup>1</sup>Department of Applied Visual Science, Graduate School of Medicine, Osaka University, Osaka 565-0871, Japan

<sup>2</sup>Research Institute, Topcon Corporation, Tokyo 174-8580, Japan

<sup>3</sup>Department of Ophthalmology, Graduate School of Medicine, Osaka University, Osaka 565-0871, Japan

<sup>4</sup>Department of Anesthesiology, Graduate School of Medicine, Osaka University, Osaka 565-0871, Japan

(Received September 7, 2006; Accepted March 8, 2007)

The purpose of this paper was to investigate the feasibility of a newly developed hyperspectral fundus imaging camera with a liquid crystal tunable filter. The intensities of different wavelengths of light transmitted through an artery, vein, and the area surrounding these vessels and reflected out were measured, and the differential spectral absorptions were analyzed. Measurements were made from 16 normal eyes and from two artificial capillaries. The ratios of absorption ( $ROA$ ) of arteries to veins from 500 to 580 nm (range 1) and from 600 to 720 nm (range 2) were calculated. For all eyes, the  $ROA_{\text{range1}}$  was larger than  $ROA_{\text{range2}}$ . The  $ROA$  obtained from the artificial capillary filled with blood saturated with oxygen or nitrogen was similar to that of simulated data of oxy- and deoxyhemoglobin extinction rate. Most  $ROA$ s of human eyes were lower than those of the simulated data and the artificial capillaries. Oxygen saturation analysis by hyperspectral fundus imaging of retinal vessels were qualitatively in agreement with the *in vitro* analysis or simulated values. However, further improvements are necessary to evaluate the oxygen saturation quantitatively in the retinal blood vessels. © 2007 The Optical Society of Japan

**Key words:** hyperspectral imaging, absorption, optical density, oxygen saturation, liquid crystal wavelength tunable filter

## 1. Introduction

The measurement of the oxygen saturation in blood is based on the principle that the extinction properties of oxy- and deoxyhemoglobin ( $HbO_2$ ,  $Hb$ ) are different in the visible and infrared spectral range. Because of this difference, spectral imaging has been used to investigate the oxygen saturation of the blood in vessels of the brain and skin.<sup>1,2</sup> For the eyes, the oxygen saturation in the retinal blood vessels has been estimated.<sup>3–6</sup> Thus, Dinn *et al.* analyzed oxygen saturation using a new method with an innovative optical density calculation using eight bit digital image and suggested that the new method could use for retinal oximetry,<sup>4</sup> while Yoneya *et al.* analyzed oxygen saturation in patients with central retinal vein occlusion (CRVO) using Fourier transform-based spectral retinal imaging and showed the oxygen saturation level was correlated with the severity of CRVO.<sup>5</sup> Delori developed a retinal vessel oximeter using a scanning fundus camera to measure optical density of a retinal vessel,<sup>6</sup> and Khoobehi *et al.* evaluated oxygen saturation in the retinal vessels using a prism-grating-prism architecture and found that pure oxygen increased oxygen saturation in veins and increasing intraocular pressures reduced oxygen saturation in the vessels.<sup>7</sup>

Recently, hyperspectral or multispectral imaging has been used in various fields. One of the novel components of this imaging system is a liquid crystal wavelength tunable filter (LCF). Hyperspectral imaging with a LCF has advantages

over the regular charge-coupled device (CCD) camera or other methods of spectral measurements in that a direct representation of two-dimensional images and a detailed spectral analysis with various wavelengths is possible.

Although many studies have been reported on the oxygen saturation of retinal blood, none has ever been widely used in the clinic.<sup>8</sup> The reasons for this may be that the accuracy of the measurements is not sufficient to be useful for clinical use. The purpose of this study was to determine the validity of using absorption analyses by hyperspectral imaging to determine the oxygen saturation in the blood of retinal vessels. To accomplish this, images of the retina and artificial capillaries filled with blood were obtained by the hyperspectral fundus camera, and the spectral absorption properties of the blood were analyzed.

## 2. Materials and Methods

### 2.1 Human subjects

Sixteen normal eyes of 16 normal subjects whose average  $\pm$  standard deviation (SD) ages was  $25.9 \pm 6.1$  year were studied.

The procedures used were approved by the Osaka University Institutional Review Board, and a written informed consent was obtained from all subjects after an explanation of the purpose and procedures to be used. All procedures conformed to the tenets of the Declaration of Helsinki.

### 2.2 Artificial capillaries and circulated blood

Glass tubings were filled with blood to simulate artificial

\*E-mail address: fujikado@ophthal.med.osaka-u.ac.jp

capillaries, and they were used to investigate the spectral characteristics of blood saturated and not saturated with oxygen. The glass tubings had an inside diameter of 1 mm and outside diameter of 1.4 mm. Artificial capillaries were filled with blood circulated by oxygen or nitrogen. Before performing the hyperspectral imaging, oxygen saturation of the circulated blood was measured using a blood gas analyzer (ABL800 FLEX, Radiometer A/S, Broenshoej, Denmark). One of the artificial capillary was perfused with blood aerated with 100% oxygen for 20 min, and the circulating blood was 100% saturated by oxygen. Another capillary was filled with blood aerated with 100% nitrogen for 2.5 min, and the oxygen saturation in the blood was 34.5%. The other three capillaries were filled with blood aerated with 100% oxygen for 2.5, 5, and 10 min from the left in Fig. 6, and the oxygen saturation in the blood was 65, 84, and 94% respectively.

It has been reported that oxygen saturation of the retinal arteries was from 90 to 98% and that of the retinal veins was from 60 to 70%.<sup>5)</sup>

### 2.3 Baseline data

The extinction values of HbO<sub>2</sub> and Hb in water have been reported.<sup>9)</sup> We used these values to calculate simulated values of the absorption of blood and compared them with the measured absorption of the blood in the retinal vessels and artificial capillaries.

### 2.4 Hyperspectral fundus camera

Our spectral imaging apparatus consisted of a mydriasis-type fundus camera (TRC-50LX, Topcon, Tokyo, Japan), a LCF (VariSpec, CRI, Woburn, MA, USA), and a CCD camera (C8484, Hamamatsu Photonics, Hamamatsu, Japan). We always used a 35-degree field for retinal imaging.

A relay lens system was built for this study to attach the LCF and the CCD to the fundus camera shown in Fig. 1.

The halogen lamp illumination system of the fundus camera was used for the hyperspectral fundus camera. An optical wavelength filter (Asahi Spectra Co., Tokyo, Japan) was used to limit the wavelength between 500 and 720 nm. The annular stop of the fundus camera was optically conjugate with the pupil of the eye, which reduced the noise component by light entering the measuring light pathway from reflectance of the cornea and the crystalline lens. The light level was one-tenth of the maximum permissible exposure (MPE) defined in ANSI-Standard Z-136.1-2000.<sup>10)</sup>

The LCF was based on a Lyot filter and is a wavelength narrow bandpass filter. The band width was 20 nm and the response time was from 50 to 150 ms. The original Lyot filter consisted of multiple layers of uniaxial birefringence retarders and polarizers. To build the LCF, liquid crystal cells replaced the regular retarders to achieve a wavelength-tunable bandpass filter.

CCD binning was used for better sensitivity and faster acquisition of spectral images. The CCD camera had 1280 × 1024 pixels but with the 4× binning, the number of pixels became 320 × 256.

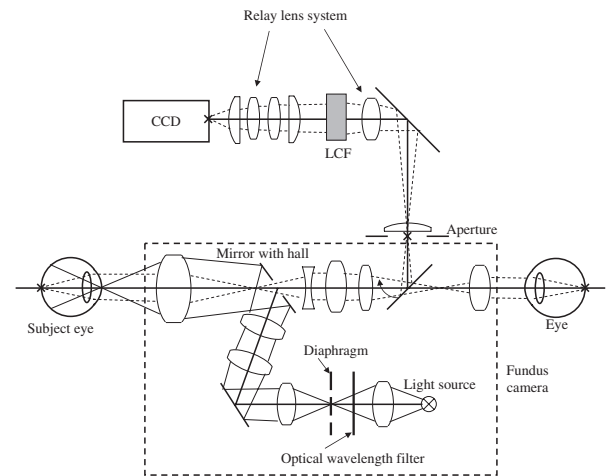


Fig. 1. Schema of optics. The spectral imaging apparatus consist of a mydriasis-type fundus camera, an LCF, and a CCD camera. Solid lines denote illumination beams and dashed lines denote imaging rays. Cross marks (x) are conjugate relations in the imaging optics.

### 2.5 Protocol of measurements

The tunable filter scanned from 500 to 720 nm, and images were obtained every 10 nm. The exposure time was 205.8 ms, and the total time to measure one eye was about 7 s. This total time was short enough for all subjects to keep their eyes open. At least two hyperspectral images were obtained from each eye, and any measurements with large displacement or noisy measurements were rejected. The averages of the multiple measurements were used for analysis.

### 2.6 Image registration and analysis of multiple images for different wavelengths

Images obtained by hyperspectral imaging shifted because of eye movements. We developed a program to register all spectral images for a series of measurements automatically to a base image, which was arbitrarily chosen. In the program, the image spectrally closest to the base image was aligned to the base image. We chose the spectrally closest image because it should resemble to the base image more than the other images (Fig. 2). The program repeated this registration. A following image, which is spectrally closest to the last registered image, would be registered as the last registered image.

To align one image on the other, the program first found a number of characteristic points on the first image. Then, it found corresponding points on the second image by a least square correlation method. Finally, the second image that was supposed to be registered was morphologically transformed by an affined transform.<sup>11)</sup>

The intensity of light reflected from the artery, vein, and the retinal area surrounding the vessels was measured, and the absorption of the blood was calculated. The vessels to be measured were selected manually, and the oxygen saturation of the vein and the artery were compared as shown in Fig. 3.

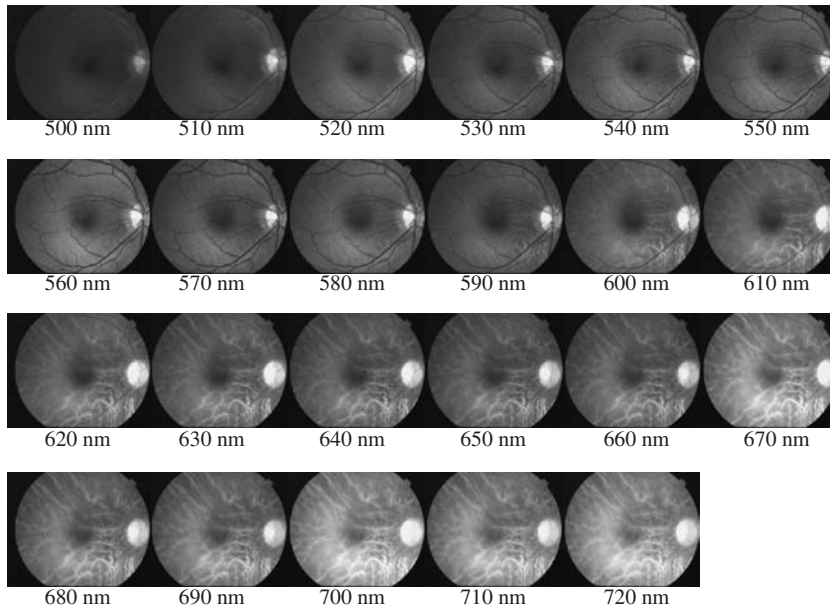


Fig. 2. Hyperspectral images of normal right eye for TM.

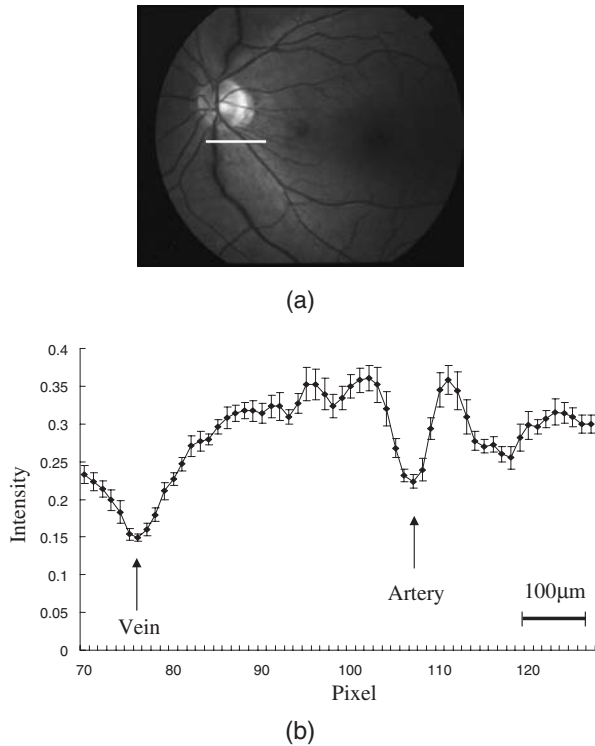


Fig. 3. Result of repeated measurements in the same wavelength. (a) Image taken by the fundus camera. The wavelength was 580 nm. The white line denotes the area analyzed. (b) Profile of the intensity. The ordinate is the intensity in the image. The unit of intensity is an arbitrary unit which the computer count normalized by its maximum value. The abscissa is the distance in pixel number. For convenience, a segment of horizontal line is shown to denote 100  $\mu\text{m}$  of the retinal length in the graph.

## 2.7 Ratio of absorptions

The ratio of the absorption (*ROA*) of arterial blood to the absorption of venous blood was used to analyze not only the

vessels in the retina but also the artificial capillaries. The analyzed data were compared with the absorption of  $\text{HbO}_2$  and Hb calculated from the reported data of  $\text{HbO}_2$  and Hb extinction values.

The optical density (*OD*) was used to investigate the absorption of arterial and venous blood. The optical density of the artery ( $OD_A$ ) and of the vein ( $OD_V$ ) at wavelength  $\lambda$  was calculated from the intensities of the light reflected from the artery ( $I_A$ ), the vein ( $I_V$ ) and the surrounding area ( $I_B$ ) using the Beer–Lambert method as follows:<sup>2)</sup>

$$OD_A(\lambda) = -\log\left(\frac{I_A(\lambda)}{I_B(\lambda)}\right) \quad (1)$$

$$OD_V(\lambda) = -\log\left(\frac{I_V(\lambda)}{I_B(\lambda)}\right) \quad (2)$$

The *ROA* at wavelength  $\lambda$  was calculated as follows.

$$ROA_\lambda = \frac{OD_A(\lambda)}{OD_V(\lambda)}. \quad (3)$$

The *ROA* over a particular spectral range was calculated as the average of  $ROA_\lambda$  over that spectral range. The *ROA* of two spectral ranges from 500 to 580 nm (range 1) and from 600 to 720 nm (range 2), were compared as follows.

$$ROA_{\text{range1}} = \frac{1}{N} \sum_{\lambda=500,510,\dots}^{580} \frac{OD_A(\lambda)}{OD_V(\lambda)} \quad (4)$$

$$ROA_{\text{range2}} = \frac{1}{N} \sum_{\lambda=600,610,\dots}^{720} \frac{OD_A(\lambda)}{OD_V(\lambda)} \quad (5)$$

These two *ROAs* for different spectral ranges were used to analyze the  $\text{HbO}_2$  and Hb.

We calculated the *ROAs* for the data of normal eyes and for the artificial capillaries.

To compare this method to method with difference of *ODs*, we calculated a quantity using a following equation for human eye measurements.

$$DOA_{\lambda} = \frac{OD_V(\lambda)}{d_V} - \frac{OD_A(\lambda)}{d_A}. \quad (6)$$

We defined the result as  $DOA_{\lambda}$ .  $d_V$  and  $d_A$  are an internal diameter of the vein and of the artery, respectively. This equation is essential and has physical meaning with Beer–Lambert law. To evaluate this equation with the measured data, we ignored the vessel diameters because we chose the measurement area where those vein and artery have almost the same diameter and we evaluated with relative values. In reality, the maximum and average of difference between them were 8.9 and 5.4% of the diameter.  $DOAs$  for range 1 and for range 2 were calculated as  $ROAs$  were calculated using eqs. (4) and (5).

We also compared our method to a method using two wavelengths for analyzing oxygen saturation. Two wavelengths we chose were 586 and 605 nm. These wavelengths were used in a previous study.<sup>4)</sup>

### 2.8 ROA obtained from reported data

$ROAs$  from the reported data were calculated by dividing the molar extinction coefficients of reported  $HbO_2$  by that of  $Hb$ . We simulated the blood in the vein with three level of oxygen saturation ratio by mixing extinction rates of  $HbO_2$  and  $Hb$  from the reported data. One of the simulations was with 100% of  $Hb$ , another was with 30% of  $HbO_2$  and 70% of  $Hb$ , and the other was with 60% of  $HbO_2$  and 40% of  $Hb$ .

Extinction rates we used for these three levels with 100% of  $HbO_2$  are shown in Fig. 5(b). We noticed that this was very simplified simulation because the binding between hemoglobin and oxygen is a complex mechanism.<sup>12)</sup> One saturated hemoglobin has four hemes which hold  $O_2$ . In the study, we ignored this and used the simplified model to investigate our method.

### 2.9 Evaluating precision of measurements

#### 2.9.1 Precision of the measurements I

We obtained retinal images on an eye with the same wavelength instead with different wavelength as in hyperspectral imaging. The fundus of a normal left eye (subject YH) was measured 20 times at 580 nm.

#### 2.9.2 Precision of the measurements II

The fundus of a normal left eye (subject TK) was measured three times from 500 to 720 nm in 10 nm steps. The results of spectral imaging were calibrated using a standard diffusing reflector. To do this, we performed hyperspectral imaging on the standard diffusing reflector immediately after measuring the eye.

#### 2.9.3 Estimation of ROA precision

We used SD of three intensity measurements from subject TK. The error propagation from the intensity measurements to  $ROA$  by optical density is as follows.

$$\Delta ROA_{\text{range1}} = \sqrt{\frac{1}{N^2} \sum_{\lambda=500,510,\dots}^{580} \left[ \left( \frac{1}{OD_V(\lambda)} \right)^2 \Delta OD_A(\lambda)^2 + \left( \frac{OD_A(\lambda)}{OD_V(\lambda)^2} \right)^2 \Delta OD_V(\lambda)^2 \right]} \quad (7)$$

$$\Delta ROA_{\text{range2}} = \sqrt{\frac{1}{N^2} \sum_{\lambda=600,610,\dots}^{720} \left[ \left( \frac{1}{OD_V(\lambda)} \right)^2 \Delta OD_A(\lambda)^2 + \left( \frac{OD_A(\lambda)}{OD_V(\lambda)^2} \right)^2 \Delta OD_V(\lambda)^2 \right]} \quad (8)$$

$$\therefore \Delta OD_A(\lambda) = \sqrt{\left( \frac{1}{I_A(\lambda)} \right)^2 \Delta I_A(\lambda)^2 + \left( \frac{1}{I_B(\lambda)} \right)^2 \Delta I_B(\lambda)^2} \quad (9)$$

$$\therefore \Delta OD_V(\lambda) = \sqrt{\left( \frac{1}{I_V(\lambda)} \right)^2 \Delta I_V(\lambda)^2 + \left( \frac{1}{I_B(\lambda)} \right)^2 \Delta I_B(\lambda)^2} \quad (10)$$

## 3. Results

### 3.1 Hyperspectral imaging

The hyperspectral images of a normal eye (right eye of subject TM) obtained with our apparatus are shown in Fig. 2. We were able to obtain clear images of normal eyes at each wavelength. The optic disc is shown as a bright round area on the right side of the image in the figures. The dark area in the center of the image is the macula. The dark lines for the shorter wavelength images (for example, in the 560 nm image) are of the retinal vessels. Because of the difference in spectral properties of the artery and vein, the vessel which had high contrast at 600 nm is the vein and the vessel which had low contrast is the artery. When the wavelength of the images becomes longer, the absorption

rate of the retina decreases. So it is easy to see the choroidal vessels which are behind the retina. Many bright choroidal vessels may be seen in images from 600 to 720 nm in Fig. 2.

### 3.2 Precision of the intensity measurements for normal eyes

#### 3.2.1 Repeated measurements at same wavelength

Figure 3(a) is the image taken by the fundus camera for left eye of subject YH. The results of repeated measurements at the same wavelength are shown in Fig. 3(b). A profile of the intensity of the fundus on the chosen line [a white line in Fig. 3(a)] including a cross section of the vein and artery is shown. The maximum SD of the multiple measurements at each point was 0.022. This maximum SD was smaller than the variation of the intensity distributed on the line. We used

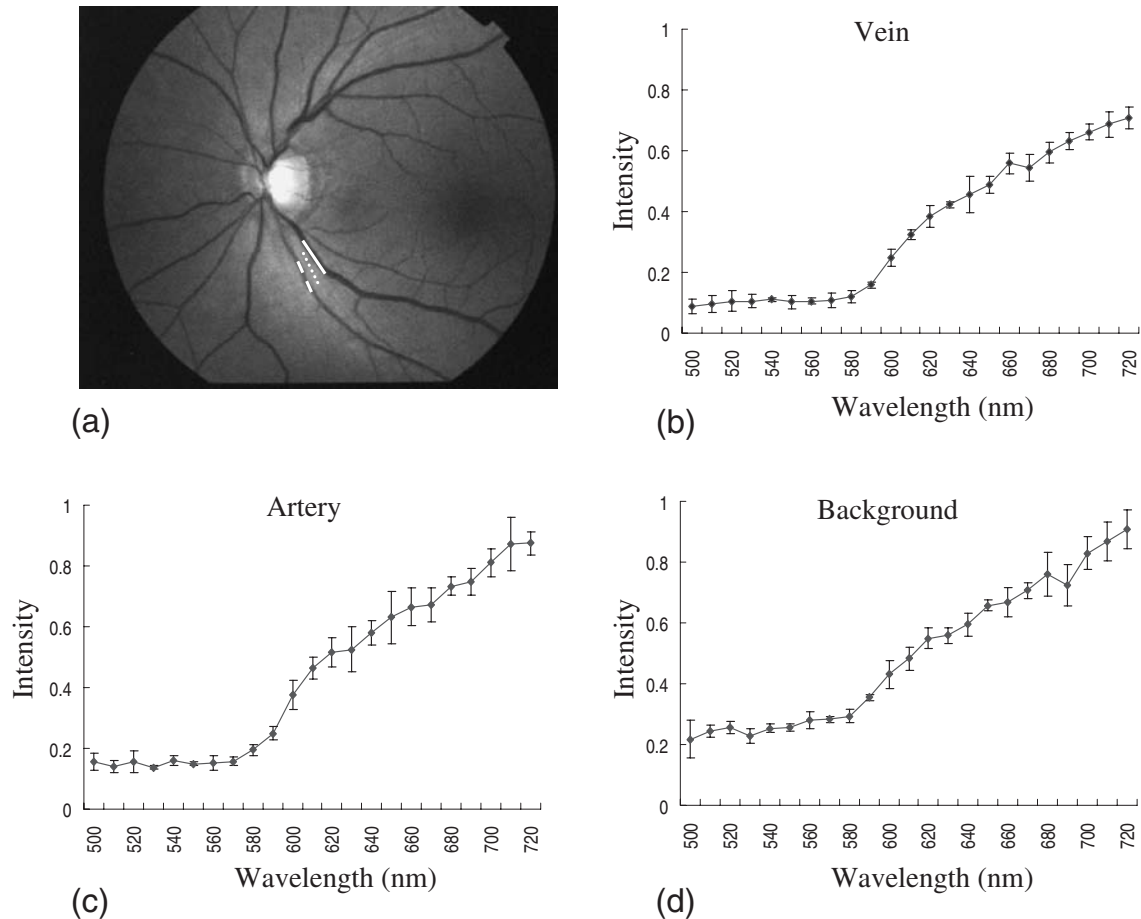


Fig. 4. Results of repeated measurements of  $I_A$ ,  $I_V$ , and  $I_B$  for all wavelength. (a) Fundus image at 580 nm and a line denoting sampling points for measuring the average intensities of the artery (dotted white line), of the vein (white line), and of the background area (small dotted white line). (b) Intensity spectral graph of the vein. (c) Intensity spectral graph of the artery. (d) Intensity spectral graph of background.

a long exposure time (205.8 ms), so any fluctuation of the intensity, e.g., by cardiovascular activity, was averaged out. We found that the reflection profile of the vein and artery had a V- or U-shaped valley with one minimum.

### 3.2.2 Repeated measurements by hyperspectral imaging

The results of repeated measurements of  $I_A$ ,  $I_V$ , and  $I_B$  for all wavelengths are shown in Fig. 4. The SDs of the intensity ranged from 0.006 to 0.059 for veins, 0.007 to 0.087 for arteries, and 0.009 to 0.072 for the background. Because the distributions of the averaged values are expressed as standard errors, we used the standard errors for estimating the precision of  $\Delta ROA_{\text{range1}}$  and  $\Delta ROA_{\text{range2}}$ .

The standard errors of  $\Delta ROA_{\text{range1}}$  and  $\Delta ROA_{\text{range2}}$  were 0.36 and 1.19, respectively. Thus, the standard error of the intensities from 600 to 720 nm was much larger than those from 500 to 580 nm. The intensity on the image of the vessel for range 2 was much closer to intensity of the background than that for range 1 (especially for vein). This caused the  $OD_V$  for range 2 to become smaller than that for range 1. And it is already known that the measurement error of intensity for range 2 is larger than that for range 1 (Fig. 4). Considering eqs. (7)–(10), this small intensity and large

error condition of intensity gave larger a error in  $ROAs$  for range 2 than that for range 1.

### 3.3 Comparison of absorption ratios

#### 3.3.1 $ROA$ from reported data

The extinction rates of  $HbO_2$  and  $Hb$  and for the simulation for other saturation levels from reported data are shown in Figs. 5(a) and 5(b).  $ROAs$  for the simulation for other saturation levels are shown in Fig. 5(c). For range 1, the extinction rates of  $HbO_2$  and  $Hb$  were not the same, but the average of the  $ROAs$  calculated from them were the same and is about 1.0. This means that  $ROA_{\text{range1}}$  does not vary even though oxygen saturation varies. The  $ROA$  decreased rapidly from 590 nm and the average of the  $ROA$  was approximately 0.2 from 600 to 720 nm. Because the intensity of an artery is always larger than that of a vein for range 2,  $ROAs$  are always less than 1.

The  $ROA_{\text{range2S}}$  for the simulate 0% of  $HbO_2$  vein blood was 0.15, the  $ROA_{\text{range2S}}$  for 30% blood was 0.2, and the  $ROA_{\text{range2S}}$  for 60% blood was 0.3. As the oxygen saturation has increased, the  $ROA_{\text{range2}}$  became larger. The  $ROA_{\text{range1S}}$  for the simulate 0% of  $HbO_2$  vein blood was 0.94. The  $ROA_{\text{range1S}}$  for 30% blood was 0.95, and the  $ROA_{\text{range1S}}$  for

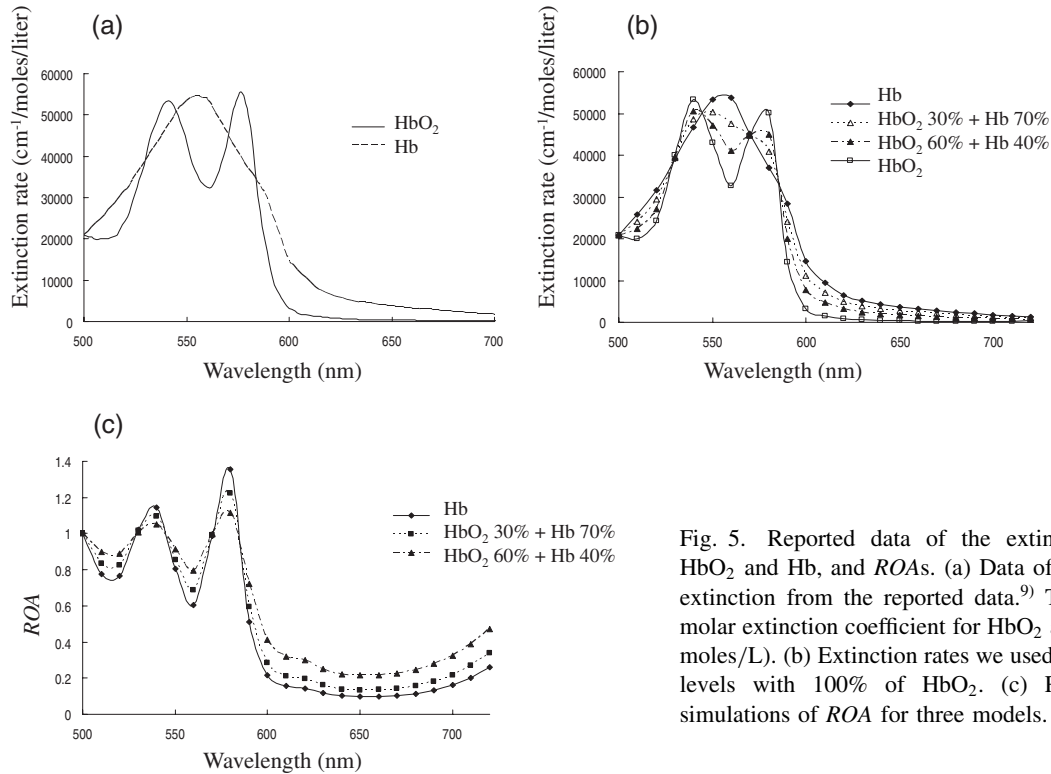


Fig. 5. Reported data of the extinction rates of HbO<sub>2</sub> and Hb, and ROAs. (a) Data of HbO<sub>2</sub> and Hb extinction from the reported data.<sup>9)</sup> The ordinate is molar extinction coefficient for HbO<sub>2</sub> and Hb (cm<sup>-1</sup>/moles/L). (b) Extinction rates we used for these three levels with 100% of HbO<sub>2</sub>. (c) Results of the simulations of ROA for three models.

60% blood was 0.96. The  $ROA_{\text{range1}}$  was always the same, regardless of oxygen saturation.

These suggested that the oxygen saturation could be estimated by  $ROA_{\text{range2}}$ , while the validity of the measurement was checked by  $ROA_{\text{range1}}$ .

### 3.3.2 ROA from artificial capillary

The images of the artificial capillaries at 580 and 640 nm are shown in Figs. 6(a) and 6(b), respectively. All of the images of the capillaries at 580 nm were dark. The image of capillaries at 640 nm was brighter for blood with higher oxygen saturation. The ROAs for the artificial capillaries [Fig. 6(c)], and tendency of the results was the same as that of the simulation from the reported data [Fig. 5(b)].

### 3.3.3 ROA from normal eyes

The ROA and the DOA for one of the subjects (left eye of subject MS) are shown in Fig. 7. This was one of the data sets where we found a problem in using DOA for our oxygen saturation level evaluation from the retinal images. The ratio of the  $ROA_{\text{range1}}$  to the  $ROA_{\text{range2}}$  was 3.01 and the ratio of the average of the DOA in range 1 to the average of the DOA in range 2 was 1.26. For DOA, the dependency on wavelength of those values was small as shown in the graph. For most eyes, ROA had larger difference between range 1 and range 2 than DOA did.

The  $ROA_{\text{range1}}$  and  $ROA_{\text{range2}}$  and ratios of the  $ROA_{\text{range1}}$  to the  $ROA_{\text{range2}}$  for reported data, capillaries, and 16 normal eyes are shown in Fig. 8. For all eyes, the  $ROA_{\text{range1}}$  was larger than  $ROA_{\text{range2}}$ . For 15 of 16 eyes, an ROA for each wavelength in range 1 was larger than that in range 2 (*t* test,  $P < 0.01$ ). These findings were the same as the reported

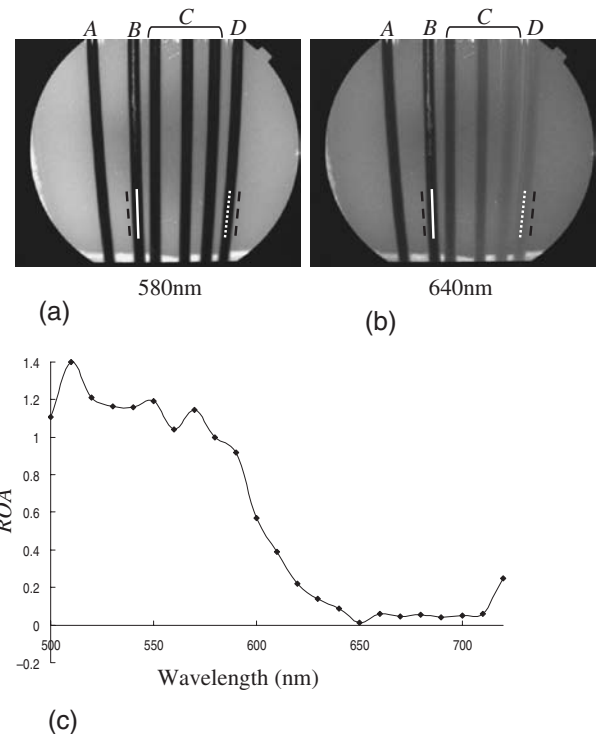


Fig. 6. Images of the artificial capillaries at 580 and 640 nm. Image of artificial capillary at wavelength 580 nm (a) and at 640 nm (b). A: Blood in capillaries were vein blood, B: nitrogen circulated blood for 2.5 min, C: oxygen circulated blood for 2.5, 5, and 10 min from the left, and D: oxygen circulated blood for 20 min. Lines are areas that were measured with the average intensities of artery (small dotted white line), vein (white line), and background area (dotted line). (c) ROA of blood circulated by oxygen or nitrogen.

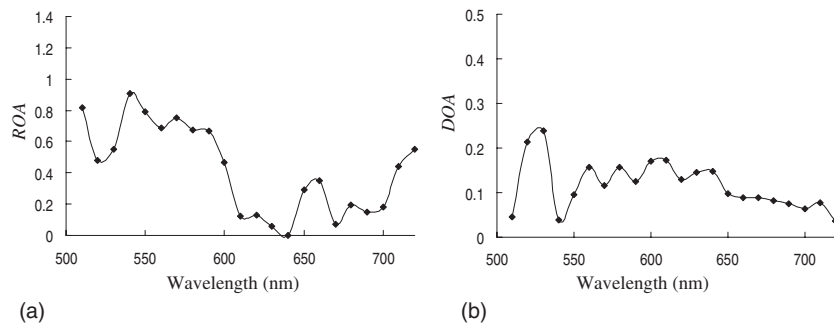


Fig. 7. Example of  $ROA$  and  $DOA$  for normal eye (left eye of subject MS). (a)  $ROA$ , (b)  $DOA$ .

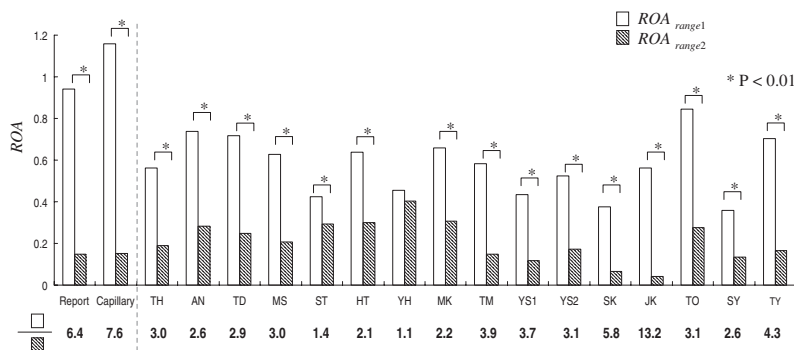


Fig. 8.  $ROA$  of range 1 and range 2 for reported data, for artificial capillary and for normal eyes. \* indicates a significant difference of  $P < 0.01$  of the comparison of each  $ROA_i$  of range 1 and those of range 2. Ratios of the  $ROA$  of range 1 to that of range 2 are shown numerically under the graph.

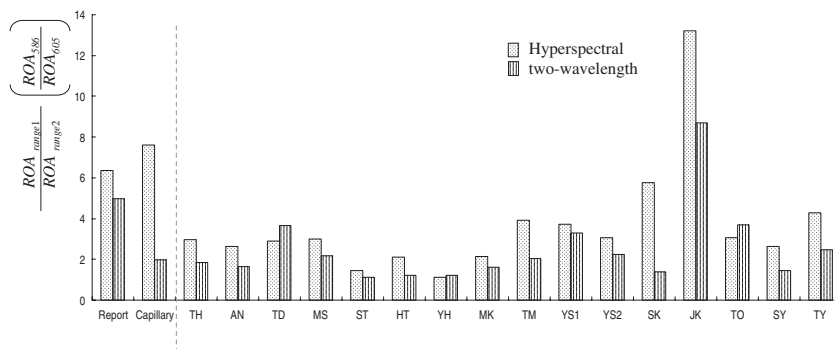


Fig. 9. The average ratio of  $ROA$  of range 1 and range 2 for hyperspectral data, and the ratio of  $ROA$  of 586 and 605 nm.

simulation data or from experiment of the artificial capillary. The average ratio of the  $ROA_{\text{range1}}$  to the  $ROA_{\text{range2}}$  for normal eyes was  $3.6 \pm 2.8$ . The ratios of the  $ROA_{\text{range1}}$  to  $ROA_{\text{range2}}$  for 15 of 16 eyes were smaller than that for the reported data and the artificial capillary.

We also compared our hyperspectral method to the method with two wavelengths for analyzing oxygen saturation. We chose 586 and 605 nm following the previous study as we described in the methods section. We calculated the ratio of absorptions for these wavelengths for direct comparison to our method. We analyzed the ratio of  $ROA_{586}$  to  $ROA_{605}$ . With the ratio of  $ROA_{\text{range1}}$  to  $ROA_{\text{range2}}$ , the results are shown in Fig. 9. Most ratios of the two-wavelength method were smaller than those of the hyperspectral method except for three cases. Because we do not know the real value of the oxygen saturation for each case, we can not conclude that the hyperspectral method is more sensitive than the two wavelength method. But, at least, we obtained different results. For example, ratio of  $ROA_{\text{range1}}$  to  $ROA_{\text{range2}}$  for subject HT was 2.1 while ratio of  $ROA_{586}$  to

$ROA_{605}$  was 1.22. Further more, noise from the cornea and the crystalline lens may be reduced with the hyperspectral method and it may be a more robust measurement.

#### 4. Discussion

Our results showed that clear and informative images can be obtained by our newly developed hyperspectral imaging fundus camera using a LCF. It required approximately 7 s to perform a hyperspectral image scan for one eye, and the duration was short enough to perform the measurements even on older patients. The ratio of the  $ROA_{\text{range1}}$  to  $ROA_{\text{range2}}$  for reported data was close to the ratio of the  $ROA_{\text{range1}}$  to  $ROA_{\text{range2}}$  of the artificial capillary. This suggests that the equipment and the analyses we used were giving valid values.

Even though the ratio of the  $ROA_{\text{range1}}$  to  $ROA_{\text{range2}}$  was close to the reported data and that of the artificial capillaries, there were still some differences. The source of the difference might have been the assumption of the simulation that neglected the complex components of blood cells.

Although the  $ROA_{\text{range1}}$  was larger than  $ROA_{\text{range2}}$  for every eye, the ratios of the  $ROA_{\text{range1}}$  to the  $ROA_{\text{range2}}$  for normal eyes were smaller than those for that of reported data and artificial capillary. This could be explained by reflection and scattering from the vessel walls, and absorption in the cornea, crystalline lens, and vitreous. For wavelengths longer than 600 nm, the light penetrates into the choroid and we observed choroidal vessels in the retinal images. Those can be a source of artifact, too.

The relative error of the results of the equation  $\Delta ROA_{\text{range1}}/ROA_{\text{range2}}$  was too large to perform accurate and precise measurements. Because the  $\Delta ROA_{\text{range2}}$  we calculated was larger than the SD of the  $ROA_{\text{range2}}$  values for all the normal subjects, we are not sure if any method using  $ROA_{\text{range2}}$  could differentiate abnormal from normal data. For spectral range 2, the choroid could influence the results because the retina is more transparent in the spectral range 2 than in the spectral range 1.

Because  $\Delta ROA_{\text{range1}}$  was smaller than the SD of  $ROA_{\text{range1}}$  values for all normal subjects, analysis with this spectral region has a potential to detect some pathological changes. In the study of Delori *et al.* and that of Khoobehi *et al.* a spectral range from 500 to 600 nm was used for oxygen saturation analysis.<sup>6,7)</sup> We believe that any method using  $ROA_{\text{range1}}$  is better than that using  $ROA_{\text{range2}}$ .

Another possible problem for hyperspectral imaging of the retina was that the cornea, the lens, and the vitreous inevitably absorb the light to be measured twice. Spectral range 1 has more absorption than range 2 in these structures.<sup>13)</sup> If there are individual variations in the spectral absorptions, we would not be able to distinguish whether the individual variation which we found in the hyperspectral imaging of the retina was caused by the eye's internal optics or by retinal components.

In conclusion, oxygen saturation analysis by hyperspectral fundus imaging of blood in the retinal vessels showed a

qualitatively consistent result with the *in vitro* analysis or simulated values. However, further improvement of the analyzing system is necessary to evaluate the oxygen saturation in the retina quantitatively.

## References

- 1) R. Frostig: in *In vivo Optical Imaging of Brain Function.*, ed. D. Boas and M. Franceschini (CRC Press, Boca Raton, FL, 2002) p. 196.
- 2) V. Tuchin: in *Handbook of Optical Biomedical Diagnostics*, ed. A. Yaroslavsky, A. Priezzhev, J. Rodriguez, I. Yaroslavsky, and H. Battarbee (SPIE Press, Washington, USA, 2003) p. 169.
- 3) A. Harris, R. B. Dinn, L. Kagemann, and E. Rechtman: *Ophthalmic Surg. Lasers Imaging* **34** (2003) 152.
- 4) R. B. Dinn, A. Harris, L. Kagemann, H. J. Garzozzi, and S. Kresovsky: Ext. Abstr. Association for Research in Vision and Ophthalmology, 2003. p. 3616.
- 5) S. Yoneya, T. Saito, Y. Nishiyama, T. Deguchi, M. Takasu, T. Gil, and E. Horn: *Ophthalmology* **109** (2002) 1521.
- 6) F. C. Delori: *Appl. Opt.* **27** (1988) 1113.
- 7) B. Khoobehi, J. M. Beach, and H. Kawano: *Invest. Ophthalmol. Vis. Sci.* **45** (2004) 1464.
- 8) H. S. Matthew, R. D. Kurt, L. Arthur, and W. H. Lloyd: *Appl. Opt.* **39** (2000) 1183.
- 9) S. Prahl (1999), <http://omlc.ogi.edu/spectra/hemoglobin/summary.html>. Oregon Medical Laser Center.
- 10) *Safe Use of Lasers* (American National Standards Institute, Orlando, FL, 2000) Z-136.1-2000.
- 11) K. Abe, Y. Tsuruga, S. Okada, T. Noma, H. Aoki, H. Fujii, H. Koike, A. Hamaguchi, and Y. Yamazaki: *Proc. SPIE* **5752** (2005) 1200.
- 12) V. W. Rodwell and P. J. Kennelly: in *Harper's Illustrated Biochemistry*, ed. R. K. Murray, D. K. Granner, P. A. Maves, and V. W. Rodwell (McGraw-Hill Medical, New York, 2003) 26th ed., p. 40.
- 13) E. A. Boettner and J. R. Wolter: *Invest. Ophthalmol. Vis. Sci.* **1** (1962) 776.